

# A Multi-modal Biometric Approach Based on Score-level Fusion and Fine-tuning Deep Learning Features

Mona Alghamdi

*School of Computing and Communications  
Lancaster University, UK*

*Department of Computer Science, Imam Abdulrahman Bin Faisal University  
Jubail, KSA*

m.alghamdi@lancaster.ac.uk; msmalghamdi@iau.edu.sa

**Abstract**—This paper presents a multimodal biometric approach applied to all fingernails and knuckle creases of the five human fingers for identifying persons. In this paper, the proposed biometric technique consists of several phases. The method starts with the detection and localisation of the main components of the hand, defining the region of interest (ROI), segmentation, feature extraction by retraining the DenseNet201 model, measuring the similarity using different metrics, and lastly, improving the person identification performance by implementing score-level fusion. This approach presents different methods for person identification, which combine fingernails, knuckles based on the modality type, and whole hands based on different similarity metrics. This paper uses various similarity metrics to distinguish between individuals. These include the Bray-Curtis, Cosine, and Euclidean metrics. Two main score-level fusion techniques are employed: the majority voting (MV) and weighted average (WA). The experimental results are evaluated with well-known databases, the '11k Hands' and the Hong Kong Polytechnic University Contactless Hand Dorsal Images 'PolyU', show the proposed algorithm's efficiency. Using the MV on the Bray-Curtis similarity measure, the fingernail-based and the base-knuckle-based fusion obtained 100% in the identification estimation. In addition, the identification rate gained 100% in regions of hands and whole hands from the two popular datasets exceeded the performance of the state-of-the-art approaches.

## I. INTRODUCTION

Typically, using personal traits such as name, position, identity card, date of birth, password, and so on to verify an individual's identity is not a suitable choice for authentication. These conventional systems have the disadvantage of being insecure and inappropriate for personal identification in the current environment [1]. It is thus important to acquire more reliable and accurate techniques for person authentication in order to control the rising crime and fraud in diverse social and commercial activities such as e-commerce, e-passport, on-line financial transaction systems, cross-border security, crime scene analysis, controlling access to restricted sites, and so on. Biometric authentication is the process of recognising a human based on their unique traits, which include physiological and behavioural qualities or both [2].

Over the past 30 years, various behavioural or physiological biometric features, such as iris, signature, hand geometry,

voice, palm print, face, and so on, have been utilised to differentiate persons in various security applications [1].

The dorsal of both right and left hands consist of several features, such as knuckle creases (including the metacarpophalangeal (MCP) joint referred as the base knuckle, the proximal interphalangeal (PIP) joint referred as the major knuckle, the distal interphalangeal (DIP) joint referred as the minor knuckle, and the interphalangeal (IP) joint referred as the major knuckle of the thumb). The hands also contain features like fingernails, unique hand shape, fingerprints, hand veins and palm creases [3].

Unimodal biometrics examples include fingerprints, DNA, finger knuckles, fingernails, hand geometry, and so on. Nevertheless, in today's digital society, there is no one biometric feature that can meet the security and performance needs of many applications [4]. Furthermore, the majority of them frequently exhibit some widely known problems such as non-uniqueness, noise in collected data, interclass similarities, non-universality, spoofing, intra-class differences, and poor discrimination capabilities. To address these issues, a multi-modal biometric system, which integrates two or more physiological or behavioural feature modalities to raise the chance of success or, more specifically, to improve the accuracy of any identification or verification application, may be a viable alternative method [1], [5].

A basic biometric system can comprise a sensor module, a feature extraction module, and a matching module. The sensor's dependability and the degrees of freedom provided by the characteristics retrieved from the detected signal heavily influence the performance of the system. For example, if the biometric feature being detected is noisy, such as a scarred knuckle, the matching score may be unreliable because a noisy input produces a high variation in the matching score. This issue can be solved by collecting various biometric features. Multimodal biometric systems are examples of such systems [6].

In this paper, a multimodal biometric approach is proposed. The approach collects various features from different sub-images of human hands. These sub-images were acquired by employing the detection and segmentation method in the study

[3]. The sub-images include fingernails, and minor, major, and base knuckles, which are fused using two major fusion rules: the MV and WA). The remainder of this paper is structured as follows: a literature review of the multi-biometric systems is in section II, the novel multimodal biometric approach from fingernail and knuckle patterns is in section III, the result and discussion are in section IV, and finally, the conclusion and recommendations for further work are in section V.

## II. MULTIMODAL BIOMETRIC SYSTEMS IN THE LITERATURE

Multibiometric systems have been developed to alleviate some of the drawbacks of unimodal authentication systems by merging data from many modalities. These systems improve the accuracy and efficiency of any identification or verification task [1]. This work [7] investigated a local textural descriptor as a binarized statistical image feature (BSIF). This feature descriptor essentially employs a series of fixed-size filters to represent the neighbourhood layout of the core pixel. Another powerful tool employed in this work was the Gabor wavelet, which has optimum localization capabilities in both the spatial and frequency domains. Furthermore, a Deep Rule-Based (DRB) classification technique was employed. The Deep Rule-Based Classifier was a process with four major phases that describe its global system mechanism [8], which included initialization, preparation, updating, and fuzzy rules generation. The authors also investigated the supply of information from different sources. The fingers' left-index-finger (LIF), left-middle-finger (LMF), right-index-finger (RIF), and right-middle-finger (RMF) modalities were merged. The studies were carried out using score-level fusion, in which the information was fused using the min-rule and the sum rule. Three experimental studies were conducted by fusing just two types of fingers, fusing three types of fingers, and fusing all sorts of fingers. The fusion was carried out with three distances (Euclidean, Cosine, and Correlation), and features were obtained using Gabor-DRB and BSIF-DRB [7].

In this study [9], using independent component analysis (ICA), a group of convolution filters were learned from the source pictures using binarized statistical image features (BSIF) (independent component analysis). A histogram of the binary codes for each pixel represents the outcomes of BSIF features. These histograms may well describe the textural elements of the photographs of the Finger Dorsal Patterns. One significant feature vector is created by combining the histograms obtained from the minor, major, and finger dorsal pattern pictures that have been encoded using the BSIF descriptor. Before the matching stage, dimensionality reduction is applied to these significant, high-dimensional vectors using a common and straightforward method called principal component analysis (PCA). The closest neighbor classifier, which employed the cosine Mahalanobis distance, was used in the matching step of the proposed system. Minimizing the distance (score) between the input query characteristic and the stored template was the standard for determining if two things were similar or dissimilar. Feature-level fusion-

extracting BSIF histograms for each of the three modalities—major, minor, and finger dorsal patterns were combined [9].

In this work [10], cascading feature extraction was applied using LBP as the beginning. The features from the relaxed local ternary pattern (RLTP) were then extracted, and a histogram of those features was created. To solve the issue of low-frequency, a uniform pattern was used to refine feature vectors. Then, dominant features were obtained using an efficient three-layered model. The investigation was carried out through the fusion of the extracted texture features from two, three, and four fingers, which were applied to the PolyU FKP database. In this work [11], an end-to-end deep learning strategy for personal identification based on minor, major, and base knuckle regions was developed. The faster region-based CNN model was used to detect the three knuckle areas, which were subsequently subjected to an automated quality check procedure. Following that, the deep distinguishing features were retrieved with the pretrained DenseNet201 model. Finally, the cosine distance was used during the matching stage. The three types of knuckles were calculated holistically using score-level fusion, and averaging rule. The offered approach was evaluated using the '11k Hands', and 'PolyU' databases [11].

Using palm-print and finger knuckle pattern finger knuckle-print (FKP) modalities at matching score-level fusion, a quick and easy hand-based recognition multimodal biometric system was developed [12]. In this study [12], the PCANet deep learning method was employed to extract the features, and a multiclass support vector machine (SVM) was applied to calculate a matching score. Also, the multiplication, sum, max, and min rules for matching score fusion were used [12].

The suggested approach in this study [13] began by separating two components: light and reflectance. First, the adaptive single-scale retinex (ASSR) technique was used to compute these components from the major or minor ROI image. Then, using Independent Component Analysis (ICA), binarized statistical image features descriptor (BSIF) trained an ensemble of convolution filters from the original images. Also, the major and minor pixels taken from dorsal finger images and reflectance and illumination images were coded using these learnt filters [13]. Finally, the fusion technique was based on the minor and major dorsal finger scores level fusion [13]. However, there is a lack of studies investigating the fusion of the dorsal hands from red-green-blue (RGB) images of all fingernails, knuckle creases, and whole hands. Also, to our knowledge, no current work studies fusion with different similarity metrics and fusion rules.

### A. Contributions and outline of this paper

The following are summaries of the paper's contributions:

- 1) To the best of our knowledge, this is the first study for person identification of the entire hand, using a holistic matching technique applied in sub-images of different knuckles and fingernails from all five fingers of both hands, resulting in an improved identification.

- 2) The fusion of Bray-Curtis, Cosine, and Euclidean difference similarity metrics has been investigated, which has not been explored in the literature.
- 3) Applying different score-level fusion techniques, such as the MV and WA, show more robust and accurate identification.

### III. THE NOVEL MULTIMODAL BIOMETRIC APPROACH

This paper presents a multi-biometrics system that is efficient, based on the score-level fusion of the fingernails, minor, major and base of the dorsal finger knuckles from five fingers of the left and right hands. Figure 1 depicts an overview architecture of the suggested approach.

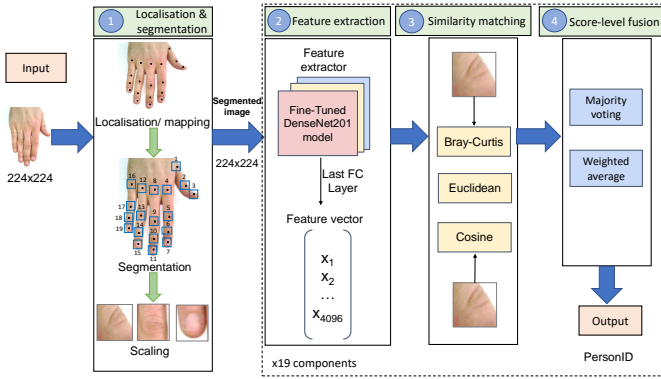


Fig. 1: A schematic illustration of the proposed fusion-based approach for identifying people using dorsal fingernails and knuckle patterns

This approach was divided into four major phases: localisation, detection, defining the region and segmentation; retraining of deep learning for feature extraction; employing similarity metrics to discover the best matching; and multi-modality score-level-based fusion.

#### A. Pre-processing of the hand images

The first stage of this work was to detect, localise, segment, normalise the base, minor, and major knuckle joints, and fingernails using the well-known multi-view bootstrapping [14] for hand posture estimation from the RGB hand image. Also, in this work, we followed the same method as explained in [3]. The output of this phase was sub-images of hand joints. The original image of the hand was scaled to 224 x 224 to achieve the best localisation performance. The detected joints were then scaled to the original high-definition image to create a larger-sized segmented image. We followed the same segmentation method offered in [3]. Following segmentation, the sub-image data was transferred to a standard scale as part of data preparation, referred to as normalisation.

#### B. Retraining deep learning for extracting features

The proposed approach's second phase was to extract high-level features by retraining the DenseNet201 deep learning algorithm. The choice of this model resulted from many evaluations applied to various deep learning models and showed outstanding performance. Therefore, we retrained the

DenseNet201 and utilised the same structure suggested in this study [15]. The very first 700 layers of DenseNet201's initial model were frozen. Then we included 2D global average pooling, batch normalisation at 0.90 momentum, dropouts at 0.5, dense layer containing 4096 vectors, a Relu activation function, 0.6 dropouts, batch normalisation with 0.9 momentum, and a 170-dimensional classifier and softmax activation function. This model was trained across a period of 150 epochs. The learning strategy was stochastic gradient descent, with a learning rate of 0.001, a Nesterov momentum of 0.9, and a loss function of categorical cross-entropy. Finally, after 100 epochs, the model was trained with all its layers and parameters [15].

#### C. Similarity metrics

The third stage was to distinguish between individuals based on similarity metrics, as displayed in figure 1. These metrics can be implemented using the extracted features from the segmented joints and are quite valuable in identifying individuals in multi-biometric systems. This paper presents three metrics: the Bray-Curtis, Cosine, and Euclidean distances. The similarity metric is the inverse of the distance metric. Assume we have two segments,  $x$  and  $y$ . Their vectors are denoted by  $x = (x_1, x_2, \dots, x_p)$  and  $y = (y_1, y_2, \dots, y_p)$ , respectively. The following section provides a brief description of the similarity metrics used in this work:

*Bray-Curtis metric* (BC) [16] is a statistical measure used to assess the distance between pairs of feature vectors. It can be described as the following equation:

$$d_{BC}(x, y) = \frac{\sum_{i=1}^P |x_i - y_i|}{\sum_{i=1}^P |x_i + y_i|} \quad (1)$$

*Cosine metric* (Cos) is another metric, which can be employed to measure the distance between two feature vectors, and uses the following function [17]:

$$Cos(x, y) = \frac{x \cdot y}{\|x\| \|y\|}, \quad (2)$$

where  $x$  and  $y$  denote vectors for which a distance is to be computed. The scalar (dot) product is also used in the numerator.

*Euclidean metric* ( $E$ ) is the most popular distance measure, which can measure the dissimilarity between two feature vectors of any pair of sub-images [17]. The Euclidean equation can be identified as follows (3):

$$E(x, y) = \sqrt{(x_1 - y_1)^2 + (x_2 - y_2)^2 + \dots + (x_n - y_n)^2} \quad (3)$$

The inverse of the distance or dissimilarity between two feature vectors is the degree of similarity. The greater the degree of similarity (Sim), the shorter the distance (Dis) between two vectors, and vice versa, as indicated by:

$$Sim(x, y) = 1 - Dis(x, y) \quad (4)$$

#### D. The score-level fusion

“Ensemble” algorithms are widely used to optimise an overall performance in the multimodal paradigm [17], [18]. In this work, two ensemble rules were utilised: the MV and WV. These algorithms optimise the overall performance of several sub-models of DenseNet201 trained in various sub-images from different hand joints. The ensemble mechanism was applied in the similarity prediction of the sub-models. In the MV, the number of modalities from hand joints from each similarity metric should be odd to avoid a tie between the estimated subject [18], otherwise the first vote has a major factor. In this paper, 19 separate hand components and three similarity matches were used in the ensemble mechanism.

1) *Majority voting (MV)*: The MV was applied on various hand components and similarity metrics. The voting system was based on the models’ estimated probability. The components representing the number of voters should be odd to avoid a tie between projected class labels [18]. As a result, an odd number of models (five) were employed. For example, five fingernails, five major knuckles or five base knuckles, except the minor knuckles, are four. In the latter case, when the votes are equal between voters, the first vote wins.

2) *Weighted average (WA)*: The WA [19] of matching data  $(m_1, m_2, \dots, m_n)$  with corresponding non-negative weights  $(w_1, w_2, \dots, w_n)$ , where  $n$  indicates the total number of subjects, is formalised as:

$$WA = \frac{\sum_{p=1}^n w_i m_i}{\sum_{p=1}^n w_i} \quad (5)$$

which includes:

$$WA = \frac{w_1 m_1 + w_2 m_2 + \dots + w_n m_n}{w_1 + w_2 + \dots + w_n} \quad (6)$$

As a result, high-weighted samples contribute more to the WA than low-weighted data samples. Negative weights are not permitted.

When the weights are normalised, they add up to one  $\sum_{n=1}^n w_i = 1$  [18]. The weight values were pre-defined based on the results of rank-1 for each component.

## IV. EXPERIMENTAL RESULTS AND EVALUATION

This section presents the results of the proposed approach’s evaluation on the datasets ‘11k Hands’ and ‘PolyU’.

#### A. Datasets description

First, we utilised the ‘11k Hands’ dataset [20], which contains RGB images with a dimension of  $1600 \times 1200$  pixels of the dorsal and palm surface of 190 subjects’ right and left hands. In this paper, we studied the dorsal hand only. The Hong Kong Polytechnic University Contactless Hand Dorsal Images Database [21], which contains 4650 of right-hand dorsal images in a flat posture from 501 subjects, was also considered. Mobile and handheld cameras were used to capture images with the same resolution  $1600 \times 1200$  pixels. Both datasets have a slight rotated hand images. The ‘11k Hands’ dataset has blurred images, polished fingernails, and rings on some fingers.

#### B. Experimental results

This study involved the identifiability of each finger in a holistic manner that integrates the performance of all fingernails and knuckles belonging to a particular finger. The fusion approaches were conducted in various regions and similarity metrics. This comprehensive computation is accomplished by score-level fusion, including the MV and WV. The proposed multimodal biometric approach was evaluated using both datasets, the ‘11k Hands’, which was divided into ‘11k-Left’ and ‘11k-Right’, for the left and right hands, respectively, and the ‘PolyU’. The performance metric was assessed using the rank-1 recognition rate as presented in the table I (individual modalities), II (multimodal biometrics based on modality type), III (fusion of the whole hand based on the similarity metrics), and the CMC chart in the figure 2, respectively. The preprocessing was conducted on the human hands, including resizing to  $224 \times 224$ , localisation of the ROI keypoints, mapping the keypoints to the image’s original size, segmentation, and scaling as explained in subsection III-A. In the second stage, the features were extracted by retraining the CNN model of DenseNet201, as explained in the subsection III-B. Then, we divided the dataset into training, validation, and testing. The training, validation, and testing percentages were 70%, 20%, and 10%, respectively. We ensured that the subject ID sub-image was included in all ROIs; therefore, we cleaned the data and discarded the subjects with missing data. The last FC layer with 4096 dimensions is then employed to extract abstract high-level features from 19 different modalities. We used the Leave-One-Out Cross-Validation (LOOCV) evaluation method in this study because the number of images was small. Each fold in the LOOCV has only one sample, and there is no random data partitioning into training and testing. Furthermore, because the samples are independent, each prediction in the identification problem is independent of the other [22]. We consider a single subject in the query at a time (and vary this, averaging the results at the end). The remaining individuals were in the library set (also replaced one at a time). Furthermore, we have individual images of both the left and right hand and 19 ROI per image. The LOOCV was employed with three different metrics: Bray-Curtis, Cosine, and Euclidean.

The proposed approach achieved excellent results in the identification rate for individual modalities as shown in the table I, multimodal biometrics in table II, and fusion of the whole hands based on various similarity metrics as shown in table III. In general, single modalities achieved excellent results, and there are no significant differences in the performance between various metrics, as demonstrated in table I.

We evaluated also the proposed approach using the fusion of different multi-modalities. Two fusion rules were utilised: the MV and WA, which employed with the metrics and improved the results as displayed in the table II. We estimated the weight for each component of the hand based on the rank-1 accuracy in table I. The MV performed better than the WA. For example, the fingernails-based fusion and the base-knuckle-based fusion

achieved 100% in all datasets using the MV that applied on the Bray-Curtis similarity metric. Also, the cumulative matching characteristic (CMC) chart in figure 2 shows a sample result from the fingernails using the cosine metric and the MV applied in all datasets, including the holistic and individual performance of each hand’s component. It is evident from the chart that the holistic technique outperforms the performance of individual modalities.

In addition, table III displays the recognition rate for the whole hand fusion that conducted with different metrics: Bray-Curtis, Cosine, and Euclidean. We can observe from the table that the MV using all distances achieved 100% in all datasets using the Bray-Curtis metric, and the fusion results significantly improved in the left hands of the ‘11kHands’ dataset.

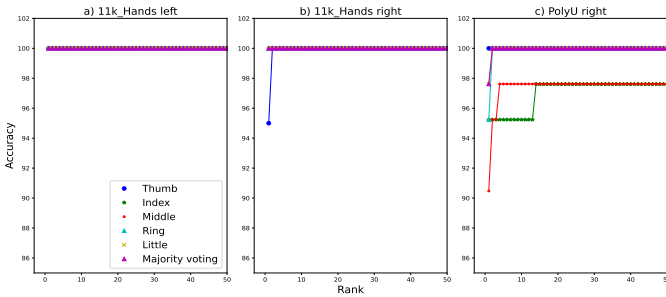


Fig. 2: The CMC diagram of the proposed fusion technique applied in the fingernails of : a) the ‘11k Hands left’; b) ‘11k Hands right’; c) ‘PolyU right’

In the next section, a comparison against the state-of-the-art approaches will be presented, and this proposed multimodal biometric outperformed them.

### C. Comparison between the proposed approach and the state-of-the-art

There is a minimal number of available studies that investigate the identification of persons using sub-images of their dorsal hands and the fusion of sub-images from the fingernails, knuckle creases, and whole hands using different similarity metrics and fusion rules. We compared our approach with the recent study in [11]. However, this paper [11] assessed the Rank-1 identification accuracy using a fusion based on the entire finger. In our proposed approach, the fusions were based on regions, e.g., the fusion of the base knuckles of fingers. In [11], the whole hand fusion techniques achieved 100%, 99.62%, and 99.33% in ‘11k-Left’, ‘11k-Right’, and ‘PolyU’, respectively. In comparison, in our study, the MV method with all metrics gained 100% using all datasets as shown in table III.

## V. CONCLUSION

To the author’s knowledge, this is the first approach for person identification that uses all fingernails and knuckle creases from human fingers. Evaluating different similarity metrics for fusion allows for solid whole-hand identification with outstanding results. Through retraining a pretrained model of

TABLE I: The rank-1 recognition rate (shown in %) for individual modalities in the ‘11k Hands’ and ‘PolyU’ datasets.

Region	Finger	similarity metric	11k-Left	11k-Right	PolyU-R
Fingernail	Thumb	Bray-Curtis	100	94.74	100
		Cosine	100	95	100
		Euclidean	100	95	100
	Index	Bray-Curtis	100	100	95
		Cosine	100	100	95
		Euclidean	100	100	95
	Middle	Bray-Curtis	100	100	90
		Cosine	100	100	90
		Euclidean	100	100	92.50
	Ring	Bray-Curtis	100	100	95
		Cosine	100	100	95
		Euclidean	100	100	95
	Little	Bray-Curtis	100	100	97.50
		Cosine	100	100	97.50
		Euclidean	100	100	97.50
Minor Knuckle	Index	Bray-Curtis	100	94.74	95
		Cosine	100	95	95
		Euclidean	100	94.74	97.50
DIP	Middle	Bray-Curtis	100	94.74	87.50
		Cosine	100	95	87.50
		Euclidean	100	94.74	87.50
	Ring	Bray-Curtis	100	100	95
		Cosine	100	95	95
		Euclidean	100	100	95
Little	Bray-Curtis	100	94.74	92.50	
	Cosine	100	95	92.50	
	Euclidean	100	94.74	92.50	
Major Knuckle	Thumb	Bray-Curtis	94.74	94.74	92.50
		Cosine	94.74	94.74	92.50
		Euclidean	100	94.74	92.50
PIP	Index	Bray-Curtis	100	94.74	97.50
		Cosine	100	94.74	97.50
		Euclidean	100	94.74	97.50
	Middle	Bray-Curtis	100	94.74	95
		Cosine	100	94.74	95
		Euclidean	100	94.74	97.50
	Ring	Bray-Curtis	94.74	94.74	92.50
		Cosine	94.74	94.74	92.50
		Euclidean	100	100	95
	Little	Bray-Curtis	100	100	97.50
		Cosine	100	100	97.50
		Euclidean	100	100	97.50
Base Knuckle	Thumb	Bray-Curtis	100	100	82.50
		Cosine	100	100	82.50
		Euclidean	100	100	82.50
MCP	Index	Bray-Curtis	100	94.74	97.50
		Cosine	100	94.74	97.50
		Euclidean	100	84.21	97.50
	Middle	Bray-Curtis	100	94.74	100
		Cosine	100	89.47	100
		Euclidean	100	94.74	100
	Ring	Bray-Curtis	100	84.21	100
		Cosine	100	89.47	100
		Euclidean	100	89.47	95
	Little	Bray-Curtis	100	100	97.50
		Cosine	100	100	97.50
		Euclidean	100	100	97.50

TABLE II: The rank-1 recognition rate (shown in %) for multimodal biometrics in the ‘11k Hands’ and ‘PolyU’ datasets.

Fusion type	Fusion rule-similarity metric	11k-Left	11k-Right	PolyU-R
Fingernails-based fusion	MV- Bray-Curtis	100	100	100
	WA- Bray-Curtis	100	99.47	96.80
	MV- Cosine	100	100	100
	WA- Cosine	100	99.40	95.48
	MV- Euclidean	100	100	100
	WA- Euclidean	100	99.37	97.30
Minor-knuckle-based fusion	MV- Bray-Curtis	100	95	93.25
	WA- Bray-Curtis	100	95	93.25
	MV- Cosine	100	95	100
	WA- Cosine	100	95	94.91
	MV- Euclidean	100	94.74	100
	WA- Euclidean	100	96.37	95.55
Major-knuckle-based fusion	MV- Bray-Curtis	95	95	97.50
	WA- Bray-Curtis	96.4	96.2	95.40
	MV- Cosine	100	94.74	97.62
	WA- Cosine	97.90	95.90	97.05
	MV- Euclidean	100	94.74	97.50
	WA- Euclidean	100	94.04	97.18
Base-knuckle-based fusion	MV- Bray-Curtis	100	100	100
	WA- Bray-Curtis	100	94.45	96.70
	MV- Cosine	100	100	100
	WA- Cosine	100	96.32	99
	MV- Euclidean	100	100	100
	WA- Euclidean	100	94.79	97.68

TABLE III: The rank-1 recognition rate (shown in %) for fusion of the whole hands based on various similarity metrics in the '11k Hands' and 'PolyU' datasets.

Similarity metric	Fusion rule	11k-Left	11k-Right	PolyU-R
Bray-Curtis	MV	100	100	100
	WA	99.64	96.67	97.73
Cosine	MV	100	100	100
	WA	99.2	96.86	97.49
Euclidean	MV	100	100	100
	WA	100	97.60	97.29

DenseNet201, the proposed approach extracts the distinctive properties of different fingernails and knuckles from the five fingers of both the right and left hands. These extracted traits are then employed with varying similarity metrics to determine the identity of all fingernails and knuckles from the five fingers and the hand as a whole. In our future work, we plan to utilise various fusion levels, including feature, score, and decision level fusion, and different rules (e.g., sum, minimum, maximum, etc.).

## REFERENCES

- [1] G. Jaswal, A. Kaul, and R. Nath, "Knuckle print biometrics and fusion schemes - Overview, challenges, and solutions," *ACM Computing Surveys*, vol. 49, no. 2, 2016.
- [2] R. de Luis-Garcia, C. Alberola-Lopez, O. Aghzout, and J. Ruiz-Alzola, "Biometric identification systems," *Signal processing*, vol. 83, no. 12, pp. 2539–2557, 2003.
- [3] M. Alghamdi, P. Angelov, and B. Williams, "Automated person identification framework based on fingernails and dorsal knuckle patterns," in *2021 IEEE Symposium Series on Computational Intelligence (SSCI)*, pp. 01–08, IEEE, 2021.
- [4] L. Hong, A. K. Jain, and S. Pankanti, "Can multibiometrics improve performance?," in *Proceedings AutoID*, vol. 99, pp. 59–64, Citeseer, 1999.
- [5] D. Lahat, T. Adali, and C. Jutten, "Multimodal data fusion: an overview of methods, challenges, and prospects," *Proceedings of the IEEE*, vol. 103, no. 9, pp. 1449–1477, 2015.
- [6] A. Ross and A. Jain, "Information fusion in biometrics," *Pattern Recognition Letters*, vol. 24, no. 13, pp. 2115–2125, 2003.
- [7] A. Attia, Z. Akhtar, N. E. Chalabi, S. Maza, and Y. Chahir, "Deep rule-based classifier for finger knuckle pattern recognition system," *Evolving Systems*, no. 0123456789, 2020.
- [8] P. P. Angelov and X. Gu, "Deep rule-based classifier with human-level performance and characteristics," *Information Sciences*, vol. 463, pp. 196–213, 2018.
- [9] A. Attia, Z. Akhtar, and Y. Chahir, "Feature-level fusion of major and minor dorsal finger knuckle patterns for person authentication," *Signal, Image and Video Processing*, vol. 15, no. 4, pp. 851–859, 2021.
- [10] M. Anbari and A. M. Fotouhi, "Finger knuckle print recognition for personal authentication based on relaxed local ternary pattern in an effective learning framework," vol. 32, p. 55, 2021.
- [11] R. Vyas, H. Rahmani, R. Boswell-Challand, P. Angelov, S. Black, and B. M. Williams, "Robust End-To-End Hand Identification via Holistic Multi-Unit Knuckle Recognition," *2021 IEEE International Joint Conference on Biometrics, IJCB 2021*, 2021.
- [12] A. Attia, "Deep learning-driven palmprint and finger knuckle pattern-based multimodal Person recognition system," pp. 10961–10980, 2022.
- [13] R. Hammouche, A. Attia, and S. Akhruf, "Score level fusion of major and minor finger knuckle patterns based symmetric sum-based rules for person authentication," *Evolving Systems*, vol. 13, no. 3, pp. 469–483, 2022.
- [14] T. Simon, H. Joo, I. Matthews, and Y. Sheikh, "Hand Keypoint Detection in Single Images using Multiview Bootstrapping," tech. rep.
- [15] M. Alghamdi, P. Angelov, and L. P. Alvaro, "Person identification from fingernails and knuckles images using deep learning features and the bray-curtis similarity measure," *Neurocomputing*, vol. 513, pp. 83–93, 2022.
- [16] R. Shyam and Y. N. Singh, "Face recognition using augmented local binary pattern and Bray Curtis dissimilarity metric," *2nd International Conference on Signal Processing and Integrated Networks, SPIN 2015*, pp. 779–784, 2015.
- [17] J. Han, M. Kamber, and J. Pei, *Data mining concepts and techniques*. Morgan Kaufmann series in data management systems, Burlington, Mass.: Elsevier, 3rd ed. ed., 2012.
- [18] G. S. Tandel, A. Tiwari, and O. G. Kakde, "Performance optimisation of deep learning models using majority voting algorithm for brain tumour classification," *Computers in Biology and Medicine*, vol. 135, no. June, p. 104564, 2021.
- [19] L. Zhang, L. Zhang, D. Zhang, and H. Zhu, "Ensemble of local and global information for fingerknuckle-print recognition," *Pattern Recognition*, vol. 44, no. 9, pp. 1990–1998, 2011.
- [20] M. Afifi, "11K Hands: Gender recognition and biometric identification using a large dataset of hand images," *Multimedia Tools and Applications*, vol. 78, no. 15, pp. 20835–20854, 2019.
- [21] A. Kumar and X. Zhihuan, "Personal Identification Using Minor Knuckle Patterns From Palm Dorsal Surface," *IEEE Transactions on Information Forensics and Security*, vol. 11, no. 10, pp. 2338–2348, 2016.
- [22] T.-T. Wong, "Performance evaluation of classification algorithms by k-fold and leave-one-out cross validation," *Pattern recognition*, vol. 48, no. 9, pp. 2839–2846, 2015.